

# A Horizon Detection Algorithm for Maritime Surveillance

Zardoua Yassir<sup>1</sup>, Astito Abdelali, Boulaala Mohammed

*Laboratory of Informatics, Signals, and Telecommunication, Faculty of Science and Technology, Tangier, Morocco*

**Abstract** The horizon line is a valuable feature in the maritime environment as it has a high persistence when compared to other features (e.g., shore corners, waves). It is used in several applications, especially in maritime surveillance. The task of horizon detection may be easy for humans, but it is hard on computers due to the high change of color and texture on maritime scenes. Moreover, the computational complexity is an important constraint to take into account while developing the algorithm. In this paper, we propose a new method that we expect to enhance the state-of-the-art.

## 1 Introduction

Nowadays, oceans host a significant number of essential human activities, which include many areas such as transportation, fishing, scientific research and more. Such activities are in a constant increase, especially in terms of trade activities [1, 2]. This implies the occurrence of threats, not only in waters but in coastal regions as well. Thus, many surveillance systems have been deployed for security purposes.

Surveillance systems usually fuse information collected from different sources. The visual data (i.e. images or video) provided by EO (Electro Optical) sensors have a significant contribution in preventing a number maritime threats. There are many commercial systems integrating these sensors [3, 4, 5, 6, 7]. The captured frames or the video is typically used to detect and track targets. This can be useful in many ways, particularly in the detection of illegal activities and prevention of collisions.

Given the high dynamicity of the maritime environment, this task is not as straightforward as it seems. Most of algorithms in the literature consider the horizon as an important feature to use as a reference, as it has a persistent presence as compared to other references. The horizon is basically defined as the boundary separating the sky region and the region right above it, which could be shore, coast, or sky region. This definition can be subject to slight changes across published papers in this field. Horizon detection algorithms can be classified in three major categories: edge-based, regional-based, and machine learning-based methods.

After an extensive review of the literature [8], we found that the different methods have only partial advantages. In particular, edge-based methods [9, 10, 11, 12, 13, 14, 15] are too sensitive to faulty lines, which can have a high contrast. Thus, application of smoothing filters [13, 14, 15, 16, 16] to

remove noise becomes ineffective. Moreover, it could hurt horizon edges in degraded contrast conditions. Regional-based method rely on regional properties such as color and texture. It does not suffer from the faulty lines issue [17, 18, 19, 20], but the latter is inherited by methods incorporating the edge information [21, 22]. Moreover, the manual rules established to exploit regional features do not handle the high change of maritime scenes [23, 17, 18, 19, 20]. Machine learning methods, in particular deep learning-based methods [24, 25, 26], seem to perform the best but require labeled samples and suffer from requiring expensive computations. Our survey [8] concludes that Jeong et al.’s method [26] is the best deep learning method in terms of balancing the trade-off between the robustness and computational load.

Given earlier discussion, our method builds on [26] to enhance its performance while bearing in mind the computational load. We note that core ideas of the method proposed in this paper are a subset of future research directions suggested in survey [8]. The rest of this paper is organized as follows. Section 2 describes the different components of our method. This section is divided into several subsections illustrating each a given component of our algorithm. Section 3 exposes experimental results we obtained so far. Finally, we conclude in section 4.

## 2 Approach Description

### 2.1 LSD-Based Filter

The first step in our approach is the detection of candidate edge pixels. Typically, this is done using an edge detector (e.g., Canny, LoG), followed by a filter, which usually relies on smoothing (e.g., mean, median). This usually hurts horizon edges in contrast-degraded conditions. Our candidate detector first applies an LSD algorithm to detect line segments, which we denote by set  $S^a$ . A good choice of Canny’s thresholds allows increasing true positives (TPs) on low-contrast images. Segments  $S^a$  pass through three stages to get candidate edge pixels. The first stage is the length-slope filter (LSF), which first removes segments whose slope  $\alpha$  satisfy  $|\alpha| \geq \alpha_{th}$ . Produced segments  $S^b$  are further filtered by taking only the longest  $N^c$  and  $N^d$  segments, such that  $N^c \ll N^d$ . Thus, the output of LSF consists of two sets of segments  $S^c$  and  $S^d$ . The next stage is a region-of-interest-based filter (ROIF), which first defines a tight region of interest (TROI) to encompass each of the  $N^c$  segments in set  $S^c$ . All segments in  $S^d$  whose endpoints fall outside defined ROIs are filtered out. Evaluating the inclusion of a segment to a given TROI can be done in several ways. The best way we found so far considers that a segment is inside a given TROI if both vertical distances, measured from endpoints of the candidate segment to the line crossing both endpoints of the segment around which the tight ROI is defined, are smaller than a threshold. Otherwise,

the segment is eliminated. Both LSF and ROIF are vectorized. For ROIF, we computed two matrices  $\Delta Y_s$  and  $\Delta Y_e$  containing all distances from endpoints of segments  $S^d$  to each line crossing segments in  $S^c$ .

Subsequent processing of  $\Delta Y_s$  and  $\Delta Y_e$  is as simple as comparison with a threshold and finding indexes corresponding to a logical *True* value. Thus, the output of the ROIF is the union of  $S^c$  and  $S^e$ , where the latter is the set of segments that survived the region of interest filter. Candidate edge pixels are eventually extracted from segments output by ROIF and forward to the patch extractor. We note that edge candidates that cannot be centered at patches not falling outside the image frame should be removed.

## 2.2 Patches Extractor

Each candidate point will be classified based on a  $m \times m$  patch centered at that candidate. Jeong et al [26] extracted a patch at each candidate point and classifies one patch per forward pass. Although the extraction of individual patches is highly parallelizable and can be efficiently implemented, a lot of redundant computations take place. Therefore, we used an alternative architecture (see section 2.3.1), which requires the union of patches as an input. We found two ways to extract such union [8]: (1) extract rectangular image portions containing the union of patches; (2) extract only the union of patches without any extra pixels. The latter requires a delicate modification of the sliding kernels. Thus, we adopted in this paper the first way.

## 2.3 Classification of Candidate Edge Pixels

### 2.3.1 Initial Classification

The prior classification process classifies candidate pixels into three classes: sea-sky, sea-obstacle, and neither. The neither class is directly regarded as the non-horizon class [8]. The sea-sky class is directly considered as a horizon class. In other words, the output of the initial classification process is actually: horizon, sea-obstacle, and non-horizon. The final classification stage decides about if a sea-obstacle edge pixel is a horizon or non-horizon pixel. The classifier in the initial classification stage is a CNN. Following Sermanet et al. [27], usage of FC layers is to be avoided and replaced by  $1 \times 1$  convolutional layer. This allows avoidance of redundant computations [8]. In our work, we used the MobileNetV2 architecture, which inherently uses  $1 \times 1$  convolutional layer instead of FC layer. Thus, the output of the classifier becomes adaptive to the input; one forward pass along the network yields the classification result of multiple candidate edge pixels instead of one candidate edge pixel as in [26]. This increases the computational efficiency and boosts the real time performance. Given the input forward to the classifier, which does likely contain patches not corresponding to any of the detected candidate edge pixels, it is worth to mention that the output of MobileNetV2 is further processed to extract only the indexes that correspond to candidate edge pixels. This is performed by creating a mask  $Idx_M$  whose number of rows and columns is equal to the number of candidate edge pixels along the width and height of the sub-image forward to the classifier, respectively.  $Idx_M$  is equal to logical *true* only at indexes that correspond to an actual edge pixel. Thus, the output of MobileNetV2 is processed by indexing it with  $Idx$ , which represents

indexes where  $Idx_M$  corresponds to logical *true*.

### 2.3.2 Final Classification

The final classification stage decides about the final class (i.e., horizon or non-horizon) of the sea-obstacle class. It is a rule based classifiers leveraging contextual information of edge pixels classifier in the previous stage [8]. The first step in this classifier is to count the number of collinear sea-sky edge pixels, which we denote as  $N_{ssk}$ . If  $N_{ssk} \geq Th_1$ , a set of collinear sea-obstacle points are reclassified as horizon points only if they are collinear with the  $N_{ssk}$  sea-sky points. Otherwise, they are considered as non-horizon. If  $N_{ssk} < Th_1$ , line segments representing collinear sea-obstacle points are established. The longest line segment (i.e., the line segment with the highest number of collinear sea-obstacle points) is first evaluated for the condition  $N_{sob} \geq Th_2$ , where  $N_{sob}$  represents the number of sea-obstacle edge pixels. If the condition is satisfied, this longest line segment is extended to span on the entire image and eventually considered as the horizon line.

## 2.4 Line Fitting

In this stage, we used the method adopted in [26, 25], which uses a linear curve fitting technique along with an outlier elimination process that is based on computing the distance of each horizon pixel from the fit line and eliminate points whose distance is higher than the median distance of all other horizon points. Compared to the Hough transform [28], this method is advantageous as the Hough transform's accuracy is sensitive to space discretization. Another advantage in this stage is its independence of the length feature of the horizon, which enables better performance in occlusion cases.

## 3 Experiments

We tested our algorithm against [26]. As both algorithms rely on labeled patches, we developed a software for patch collection and annotation. Instead of the random selection of patches adopted in [26], this software allowed us to collect and label a high quality dataset thanks to the special tools in developed software.

We randomly selected a set of frames from the SMD (Singapore Maritime Dataset [29]) and from our own collected dataset a set of 1000 frames. The results of horizon detection using our method and method [26] is shown in table 1. In the latter, high accuracy corresponds to cases where no observable error exist (see figure 1(a)). Medium accuracy corresponds to cases where several horizon edge pixels are correctly classified, but some misclassifications of collinear edges took place near the horizon (see figure 1(b)). A low accuracy corresponds to cases where horizon edges are either not detected or misclassified such that the detected horizon is far than the correct detection (see figure 1(c)). Table 1 shows that our method achieves the best accuracy in all qualitative metrics in comparison to [26]. In the future, we will provide experimental results on a larger number of frames with more accurate metrics: quantitative metrics measuring the average error and standard deviation error of the position  $Y$  and tilt

$\alpha$  of the horizon. We will share the results of computational speed of our algorithm and Jeong et al's [26] algorithm after the optimization of written code.

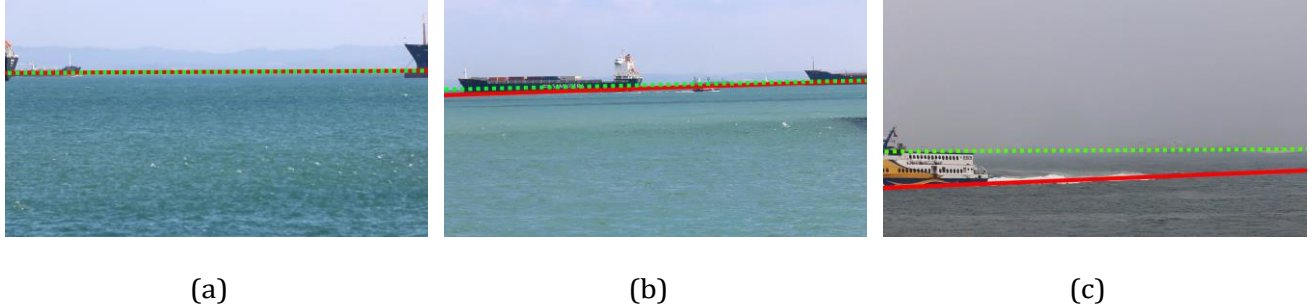


Fig.1. Illustration of the qualitative evaluation used; the red line corresponds to the detected horizon, whereas the green dashed line corresponds to the ground truth horizon; (a) high accuracy (the green dashed line is superimposed on the red line); (b) medium accuracy; (c) low accuracy

**Table 1.** Accuracy of detected horizon lines on 1000 frames

Methods	High Accuracy	Medium Accuracy	Low Accuracy
<b>Ours</b>	95.31%	3.55%	<b>1.14%</b>
<b>Jeong et al. [26]</b>	<b>83.74%</b>	<b>11.66%</b>	<b>4.60%</b>

#### 4 Conclusions

In this paper, we proposed a new method that builds on [26]. We found that our method is robust in low-contrast conditions thanks to the adopted filter used. Also, the two-stage-classification enhances the performance when the region above the horizon change its appearance (e.g., from sky to shore). This paper will be updated to include more details on our implementation and techniques described herein. Our current research focuses on extending the benchmark of the proposed algorithm by including more state-of-the art algorithms and extending the experimental results on more conditions while using more reliable evaluation metrics that measures quantitatively the accuracy of detected horizon.

## References

- [1] *Review of Maritime Transport*. un.org/publications, 2018.
- [2] Yassir Zardoua, Abdelali Astito, and Mohammed Boulaala. A comparison of ais, x-band marine radar systems and camera surveillance systems in the collection of tracking data. *International Journal of Recent Research and Applied Studies*, 7(4):1–5, 2020.
- [3] Bradley J Rhodes, Neil A Bomberger, Todd M Freyman, William Kreamer, Linda Kirschner, CL Adam, Wendy Mungovan, Chris Stauffer, Lauren Stolzar, Allen M Waxman, et al. Seecoast: persistent surveillance and automated scene understanding for ports and coastal areas. In *Defense Transformation and Net-Centric Systems 2007*, volume 6578, page 65781M. International Society for Optics and Photonics, 2007.
- [4] Kalyan Moy Gupta, David W Aha, Ralph Hartley, and Philip G Moore. Adaptive maritime video surveillance. In *Visual Analytics for Homeland Defense and Security*, volume 7346, page 734609. International Society for Optics and Photonics, 2009.
- [5] Domenico Bloisi and Luca Iocchi. Argos, a video surveillance system for boat traffic monitoring in venice. *International Journal of Pattern Recognition and Artificial Intelligence*, 23(07):1477–1502, 2009.
- [6] Hai Wei, Hieu Nguyen, Prakash Ramu, Chaitanya Raju, Xiaoqing Liu, and Jacob Yadegar. Auto- mated intelligent video surveillance system for ships. In *Optics and Photonics in Global Homeland Security V and Biometric Technology for Human Identification VI*, volume 7306, page 73061N. In- ternational Society for Optics and Photonics, 2009.
- [7] Nuno Pires, Jonathan Guinet, and Elodie Dusch. Asv: an innovative automatic system for maritime surveillance. *Navigation*, 58(232):1–20, 2010.
- [8] Yassir Zardoua, Abdelali Astito, and Mohammed Boulaala. A survey on horizon detection algorithms for maritime video surveillance: advances and future techniques. *The Visual Computer*, pages 1–21, 2021.
- [9] Evgeny Gershikov, Tzvika Libe, and Samuel Kosolapov. Horizon line detection in marine images: which method to choose? *International Journal on Advances in Intelligent Systems*, 6(1), 2013.
- [10] Evgeny Gershikov. Is color important for horizon line detection? In *2014 International Conference on Advanced Technologies for Communications (ATC 2014)*, pages 262–267. IEEE, 2014.

- [11] Gui-Qiu Bao, Shen-Shu Xiong, and Zhao-Ying Zhou. Vision-based horizon extraction for micro air vehicle flight control. *IEEE Transactions on Instrumentation and Measurement*, 54(3):1067–1072, 2005.
- [12] Tomasz Praczyk. A quick algorithm for horizon line detection in marine images. *Journal of Marine Science and Technology*, 23(1):164–177, 2018.
- [13] Yu-Fei Shen, Zia-Ur Rahman, Dean Krusienski, and Jiang Li. A vision-based automatic safe landing- site detection system. *IEEE Transactions on Aerospace and Electronic Systems*, 49(1):294–311, 2013.
- [14] Yu-Fei Shen, Dean Krusienski, Jiang Li, and Zia-ur Rahman. A hierarchical horizon detection algorithm. *IEEE Geoscience and Remote Sensing Letters*, 10(1):111–114, 2012.
- [15] Dilip K Prasad, Deepu Rajan, Lily Rachmawati, Eshan Rajabally, and Chai Quek. Muscowert: multi-scale consistence of weighted edge radon transform for horizon detection in maritime images. *JOSA A*, 33(12):2491–2500, 2016.
- [16] Chi Yoon Jeong, Hyun S Yang, and KyeongDeok Moon. Fast horizon detection in maritime images using region-of-interest. *International Journal of Distributed Sensor Networks*, 14(7):1550147718790753, 2018.
- [17] Bahman Zafarifar, Hans Weda, et al. Horizon detection based on sky-color and edge features. In *Visual Communications and Image Processing 2008*, volume 6822, page 682220. International Society for Optics and Photonics, 2008.
- [18] Steven J Dumble and Peter W Gibbens. Horizon profile detection for attitude determination. *Journal of Intelligent & Robotic Systems*, 68(3-4):339–357, 2012.
- [19] Terry Cornall and Greg Egan. Calculating attitude from horizon vision. In *Eleventh Australian International Aerospace Congress, Melbourne*, 2005.
- [20] Terry Donald Cornall, Gregory Kenneth Egan, and A Price. Aircraft attitude estimation from horizon video. *Electronics Letters*, 42(13):744–745, 2006.
- [21] Sergiy Fefilatyev, Dmitry Goldgof, Matthew Shreve, and Chad Lembke. Detection and tracking of ships in open sea with rapidly moving buoy-mounted camera system. *Ocean Engineering*, 54:1–12, 2012.

- [22] Dong Liang and Ya Liang. Horizon detection from electro-optical sensors under maritime environment. *IEEE Transactions on Instrumentation and Measurement*, 69(1):45–53, 2019.
- [23] Scott M Ettinger, Michael C Nechyba, Peter G Ifju, and Martin Waszak. Towards flight autonomy: Vision-based horizon detection for micro air vehicles. In *Florida Conference on Recent Advances in Robotics*, volume 2002, 2002.
- [24] Wenqiang Zhan, Changshi Xiao, Yuanqiao Wen, Chunhui Zhou, Haiwen Yuan, Supu Xiu, Xiong Zou, Cheng Xie, and Qiliang Li. Adaptive semantic segmentation for unmanned surface vehicle navigation. *Electronics*, 9(2):213, 2020.
- [25] CY Jeong, HS Yang, and KD Moon. Horizon detection in maritime images using scene parsing network. *Electronics Letters*, 54(12):760–762, 2018.
- [26] Chiyoon Jeong, Hyun S Yang, and KyeongDeok Moon. A novel approach for detecting the horizon using a convolutional neural network and multi-scale edge detection. *Multidimensional Systems and Signal Processing*, 30(3):1187–1204, 2019.
- [27] Pierre Sermanet, David Eigen, Xiang Zhang, Michaël Mathieu, Rob Fergus, and Yann LeCun. Overfeat: Integrated recognition, localization and detection using convolutional networks. *arXiv preprint arXiv:1312.6229*, 2013.
- [28] Paul VC Hough. Method and means for recognizing complex patterns, December 18 1962. US Patent 3,069,654.
- [29] Dilip K Prasad, Deepu Rajan, Lily Rachmawati, Eshan Rajabally, and Chai Quek. Video processing from electro-optical sensors for object detection and tracking in a maritime environment: a survey. *IEEE Transactions on Intelligent Transportation Systems*, 18(8):1993–2016, 2017.